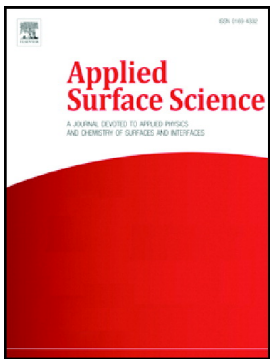

Optimization of low temperature RF-magnetron sputtering of indium tin oxide films for solar cell applications

M.G. Sousa, A.F. da Cunha

PII: S0169-4332(19)30906-7
DOI: https://doi.org/10.1016/j.apsusc.2019.03.275
Reference: APSUSC 42230

To appear in: *Applied Surface Science*

Received date: 3 December 2018
Revised date: 17 March 2019
Accepted date: 24 March 2019

Please cite this article as: M.G. Sousa and A.F. da Cunha, Optimization of low temperature RF-magnetron sputtering of indium tin oxide films for solar cell applications, Applied Surface Science, https://doi.org/10.1016/j.apsusc.2019.03.275

Optimization of Low Temperature RF-magnetron sputtering of Indium Tin Oxide Films for Solar Cell Applications

M.G.Sousa[a,*], A.F. da Cunha[a]

[a]*I3N and Physics Department, University of Aveiro, 3810-193, Aveiro, Portugal*

Abstract

In this work we have studied the influence of argon working pressure, substrate temperature, low power plasma irradiation and partial pressure of hydrogen in the RF-magnetron sputtering of indium tin oxide (ITO) thin films on glass substrates. This work aims at identifying the best conditions to achieve good quality ITO films at low temperature for deposition on heat-sensitive substrates. Four sets of samples were prepared which were characterized by X-ray diffraction (XRD), Van der Pauw and transmittance measurements. It was found that structural, electrical and optical properties of the films depend strongly on the deposition parameters. ITO films with a thickness of $\sim$ 300 nm, displaying a sheet resistance of 68 Ω/sq and average transmittance, in the visible range, of about 90% were produced performing the deposition at low pressure and at room temperature. However, further improvements in the sheet resistance up to a factor of 3 were obtained by decreasing a little more the argon working pressure or applying a low power plasma irradiation or adding a partial pressure of hydrogen to the working gas. Films produced at low working pressures are crystalline and have [222] preferential orientation. The conductivity and transmittance of these films are higher than those of films deposited at high pressures. The electrical resistivity of the ITO thin films decreased sharply either with low power plasma irradiation or the addition of a partial pressure of H_2 to the working gas. All the films showed an average transmittance of over 80% in the visible range. Therefore, as a result of this work we established that the addition of a small partial pressure of H_2 to the working gas during growth allowed us to achieve the main aim of depositing low resistivity ITO films at low substrate temperature suitable for the envisaged applications. At the same time, we concluded that this approach leads to a drastic reduction in the amount of target surface conditioning required every time a new target was installed because it turns the properties of the ITO films more independent of the target surface properties.

Keywords: Indium Tin Oxide (ITO), RF-magnetron sputtering, Argon working pressure, Substrate temperature, Plasma irradiation, Partial pressure of hydrogen

1. Introduction

Significant advances have been taking place in the field of semiconductor physics during the past few decades because of their numerous pratical applications. One of the most important fields is the fundamental aspects and applications of semiconducting transparent thin films. Such materials are highly conducting and exhibit high transparency in the visible region of the electromagnetic spectrum [1]. Because of this unique property, transparent conducting oxides (TCOs) are finding a large range of applications in research and industry [1, 2]. For the purpose of the present work, the application of concern are photovoltaic cells and improvement in performance of the TCOs is important because their non-ideal properties will eventually impact the performance of the complete device [1].

A TCO is a wide band gap semiconductor that has high concentration of free electrons in the conduction band, either from defects in the material or from dopants and, where the impurity levels of which lie near

*Corresponding author
Email address: martasousa@ua.pt (M.G.Sousa)

the conduction band (CB) edge (an n-type material) [1, 2]. The high electron carrier concentration causes absorption of electromagnetic radiation in both visible and infrared portions of the spectrum. And because a TCO must represent a compromise between electrical conductivity and optical transmittance, a careful balance between the properties is required. A reduction of the resistivity involves either an increase in the carrier concentration or in the mobility [3]. But the increase in the former will lead to an increase in the visible absorption while the increase in mobility has no adverse effect on the optical properties. Achieving a high carrier mobility will necessarily improve the optical properties [1]. The dominant TCOs are tin oxide (SnO_2), indium oxide (In_2O_3) and zinc oxide (ZnO). Doping these oxides (antimony or fluorine doped SnO_2 (ATO and FTO), tin doped In_2O_3 (ITO) and Al doped ZnO (AZO)) resulted in improved electrical conductivity without degrading their optical transmission. In particular, ITO is the most common TCO in the solar cell technology [4, 5, 6]. Considering our particular case study of $Cu_2ZnSn(S,Se)_4$ (CZT(S,Se)) Thin Film Solar Cells, the technological status reveal that the highest power conversion efficiencies (PCEs) are achieved when the TCO indium tin oxide is used as the window layer (Table 1).

Table 1: Technological status of $Cu_2ZnSn(S,Se)_4$ Thin Film Solar Cells.

Absorber	TCO	Technique	PCE (%)	REF
CZTS	ITO	co-sputtering	11.01	[7]
CZTS	ZnO:B	evaporation+sulfurization	9.2	[8]
CZTS	ZnO:Al	co-electrodeposition	8.7	[9]
CZTS	ZnO	coevaporation	8.4	[10]
CZTS	ITO	electrodeposition+sulfurization	8.0	[11]
CZTS	ITO	sol gel+sulfurization	5.67	[12]
CZTSe	ITO	coevaporation	11.6	[13]
CZTSe	ZnO:Al	DC sputtering+selenization	9.7	[14]
CZTSe	ITO	nanoparticles+selenization	9.3	[15]
CZT(S,Se)	ITO	hydrazine+selenization	12.6	[16]
CZT(S,Se)	ZnO:Al	ink+selenization	9.02	[17]
CZT(S,Se)	ITO	sol gel+selenization	8.25	[18]
CZT(S,Se)	ZnO:Al	ESAVD+selenization	6.35	[19]
CZT(S,Se)	ITO	hydrazine+selenization	12.7	[20]

Tin doped indium oxide (indium tin oxide or ITO) is a n-type degenerated semiconductor with a band gap $\sim$ 3.75 eV, low resistivity ($< 5x10^{-4}$ Ωcm) and a work function of 4.8 eV [2, 4]. It has high conductivity and transparency in the visible range of the spectrum and high reflectance in the infrared range. This material offers best available performance in terms of conductivity ($\sim 10^3$ - 10^4 $\Omega^{-1}cm^{-1}$) and transmitivity ($\sim$ 95%) combined with excellent reproducibility, environmental stability, good surface morphology and excellent substrate adherence [1, 4]. These two properties (transparency and conductivity) are interrelated and it is hard to improve one without reducing the other and the optimal value is often a compromise. The low resistivity of ITO films has been attributed to excessive number of free electrons ($> 10^{20}$ cm^{-3}) causing the Fermi level to be located in the CB, due to both substitutional tin atoms incorporated during deposition and oxygen vacancies that are created during deposition [2]. Its transparency in the visible region is due to its allowed direct transition wide band gap [2]. All these reasons, make ITO, a key part of solar cells and improving the ITO layer can help to improve the solar cell efficiency [21].

ITO is essentially formed by substitutional doping of In_2O_3 with tin, which replaces the In^{3+} atoms. Tin thus forms an interstitial bond with oxygen and exists either as SnO or SnO_2, accordingly it has a valency of +2 or +4, respectively. This valency state has a direct bearing on the ultimate conductivity of ITO. The lower valence state results in a reduction in carrier concentration, since a hole is created which acts as a trap and reduces conductivity. On the other hand, prominence of the SnO_2 state means Sn^{4+} acts as an n-type donor releasing electrons to the conduction band. However, in ITO, both substitutional tin and oxygen vacancies contribute to the high conductivity [3, 22, 23].

Various deposition techniques, such as, spray pyrolysis [24], chemical vapour deposition (CVD)[25], evaporation in reactive atmosphere or vacuum [5, 26], DC magnetron reactive sputtering [27, 28], RF sputtering [28, 29], electron beam evaporation [22] and pulsed laser deposition [30] were used to deposit ITO thin films. Among these technologies RF-magnetron sputtering technique is the most suitable method for ITO deposition on large area thin film optoeletronic devices [4]. However, almost all the reported ITO films were fabricated at rather high temperature, also because of the high fabrication temperature. Even though some materials are deposited onto very hot substrates, others must be deposited onto heat-sensitive substrates. In addition, thin film solar cells, based on CIGS or CZTS, for example, the ITO is the last layer deposited and its deposition temperature must be compatible with the semiconductor layers already deposited, otherwise, interdiffusion of layers can occur, thereby ruining the device performance. The interfaces of the ITO and the other layers of the devices must be stable and with a low specific contact resistance, considering the importance of this layer in thin film solar cells, to contribute to the transmission of the light to the absorber and to transport the photocurrent with the lowest possible ohmic losses. Therefore, it is very necessary to study the ITO films deposited at low processing temperatures. To that end, the deposition conditions much necessary to produce ITO films with high conductivity and optical transparency were studied and optimized. ITO films have been deposited by RF magnetron sputtering and the influence of argon working pressure, substrate temperature, low power plasma irradiation and partial pressure of hydrogen on the structural, electrical and optical film properties is reported. A strong dependency of the films' properties on the set of growth parameters is observed.

2. Experimental methods

Indium tin oxide thin films were deposited on glass substrates by RF magnetron sputtering. The substrates with 3x3 cm^2 were cleaned in successive ultrasound baths of acetone/ethanol/deionized water, rinsed with the latter, dried in nitrogen and were kept in a load lock chamber. The system is pumped down to a pressure of $\sim$ 2.0x10^{-7} Torr prior to deposition in vacuum. Under these conditions the samples are transferred to the deposition chamber above the target at a distance of $\sim$ 10 cm. The ITO ceramic target used consisted of high density In_2O_3:SnO_2 in a 90/10 wt% ratio, with 99.99% of purity and 2 inches in diameter. The process is started by introducing continuous flow of argon, Ar (or Ar+5%H_2) into the deposition chamber and setting the pressure at a 10^{-2} Torr. A power of 20 W is applied to the magnetron, to ignete the plasma. Prior to the actual deposition step, 10 minutes of pre-sputtering period were allowed to clean and condition the ITO target surface. The RF power used to sputter the ITO target was then rumped up to 120 W at a rate of 0.5 W/s and just before reaching the final value the pressure was reduced to the final working pressure, in the order of 10^{-3} Torr. The actual deposition starts with opening of the substrate shutter. During the deposition the substrate holder is rotated at 5 rpm to improve the deposition uniformity. Film thickness and deposition rates ($\AA$/s) are monitored in real time using a quartz crystal sensor. The deposition time for all the studied ITO films is 50 minutes. Different deposition conditions were studied and a summary of the samples produced and the corresponding growth conditions was given in Table 2.

The films thus grown were characterized using different tools. The surface morphology and average composition were analyzed by SEM/EDS using a TESCAN Vega3 SBH SEM microscope, operated at an acceleration voltage of 15.0 kV for image acquisition and 25 kV for chemical analysis.The crystalline structure was analysed by X-ray diffraction (XRD) with a Philips PW 3710 system, in the Bragg-Brentano configuration (θ-2θ), using the CuK_α line (λ $\sim$1.54060 Å) and the generator settings were 50 mA and 40 kV. The electrical properties were studied via Hall effect measurements, performed in Van der Pauw geometry at room temperature. The optical properties were investigated using UV-VIS-NIR spectrophotometer by recording the transmission spectra. The film sheet resistance was measured with a four point probe setup.

3. Results and Discussion

The main goal of this work was to optimize the growth conditions of ITO thin films at low processing temperatures. In order to investigate the properties of ITO thin films, grown at different sputtering conditions, several characterization techniques were used and the results are presented and discussed below.

Table 2: Summary of the different sputtering process parameters studied and the corresponding name of the samples.

Samples	Argon working pressure (mTorr)	Flow Rate (SCCM)	Substrate temperature (ºC)	Plasma irradiation power (W)	Hydrogen content in the working gas (%)
ITORTp2.85	2.85	4.52 Ar	RT	NA	NA
ITORTp3.00	3.00	4.90 Ar			
ITORTp4.35	4.35	7.80 Ar			
ITORTp4.85	4.85	8.91 Ar			
ITORTp2.85	2.85	4.52 Ar	RT		
ITOT100p2.85		4.58 Ar	100		
ITOT150p2.85		4.60 Ar	150		
ITOT250p2.85		4.62 Ar	250		
ITORTp2.85P0W		4.52 Ar	RT	NA	
ITORTp2.85P10W		4.64 Ar		10	
ITORTp2.85P20W		4.56 Ar		20	
ITORTp2.85P40W		4.36 Ar		40	
ITORTp2.85P0W$H_2$0%		4.52 Ar		NA	NA
ITORTp2.85P0W$H_2$5%		2.15 Ar + 2.15 (Ar + 5%H_2)			5

* RT= Room Temperature
* NA= Not Applicable

3.1. Sctructural properties of ITO thin films

Figure 1 (a-d) shows the XRD patterns for ITO films deposited by different conditions. The diffraction patterns contain only In_2O_3 peaks corresponding to (211), (222), (400), (440) and (622) crystal planes which match well with the bixbyite tin substitued In_2O_3 structure having lattice parameter a=10.14 $\AA$ [21]. As shown in figure 1, none of the spectra indicated any characteristic peaks of Sn, SnO or SnO_2, which means that the tin atoms were probably incorporated substitutionally into the In_2O_3 lattice [21]. It is observed that all deposited ITO thin films have (222) or (400) preferred orientations, depending on the growth conditions. Decreasing argon working pressure either leads to a shift from an amorphous structure to one with a high degree of crystallinity. Also the increase in the substrate temperature or a low power plasma irradiation of the growing films improves the crystallinity. The latter promotes a shift in the preferred crystal orientation from (222) to (400) with the increase of irradiation power. These observations suggest that the structure and orientation of ITO thin films depends on the energy of the sputtered particles arriving at the substrate. The thermalized sputtered atoms are known to orient as (222) while the particles with higher energies prefer the (400) and (440) orientations [31]. The addition of 5% of hydrogen to the working gas does not substantially change the crystallinity of the films. These different results indicate that the ITO films structure orientation depend strongly on the deposition parameters.

A specific preferred orientation of a film can be discussed on the basis of strain. Crystal imperfections and distortion of strain-induced peak broadening are related by $\varepsilon=\beta_{hkl}/4\ \tan(\theta)$, according to Williamson-Hall method [32]. Increasing the argon working pressure from 2.85 mTorr to 3.00 mTorr, there is a decrease in strain from 0.3686 to 0.2899, respectively. Applying a substrate temperature of 100 °C, 150 °C and 250 °C there is no significant difference between the strain. The corresponding values are 0.3109, 0.3246 and 0.3133, respectively. However, this values are lower than the ITO film produced at room temperature, with a strain of 0.3686. This is consistent with the XRD data where the increase in the substrate temperature improves the crystallinity. The real-time in-situ controlled plasma irradiation of the growing film changed their preferred crystal orientation with the increase of irradiation power. In both cases, the increase in the irradiation power leads to a decrease in strain, and consequently an increase in the crystallinity. The samples with the (222) preferred crystallographic orientation, namely, ITORTp2.85P0W and ITORTp2.85P10W, have strain

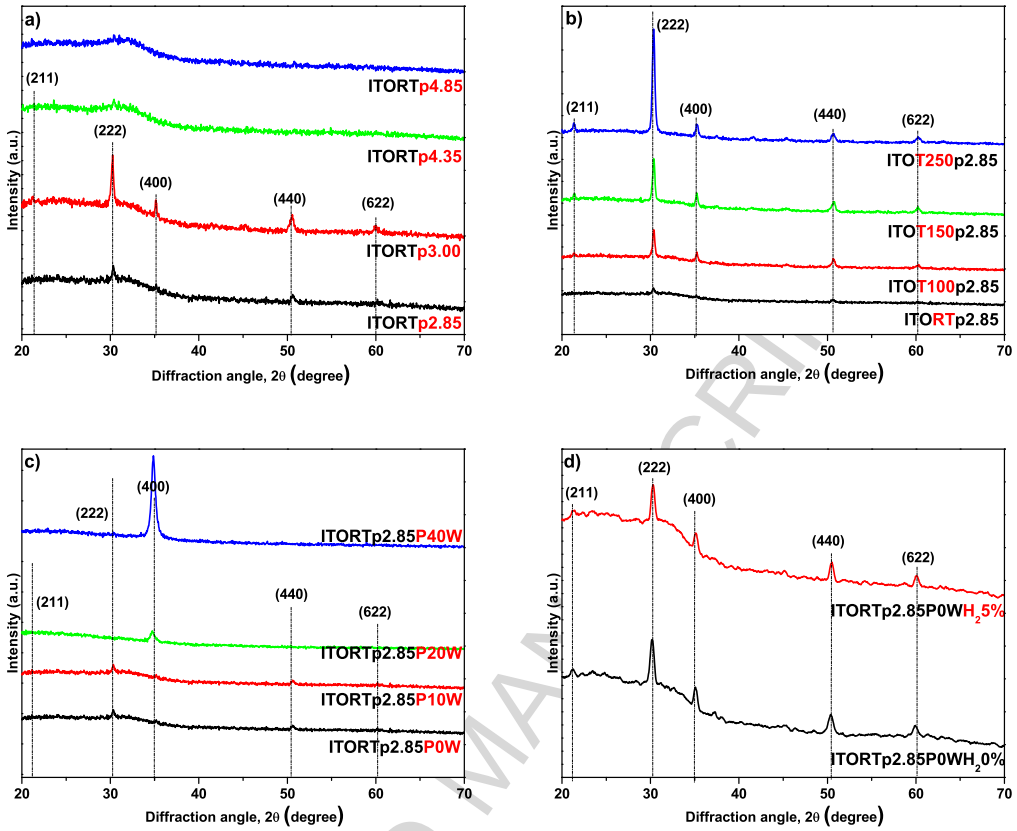

Figure 1: X-ray diffraction patterns of ITO films as a function of a) Argon working pressure; b) Substrate temperature; c) Power plasma irradiation and, d) Partial pressure of hydrogen.

values of 0.3686 and 0.2997. For plasma irradiation with 20 W and 40 W, the values vary between 0.5788 and 0.4974. Less strain (ε=0.2891) is obtained when 5% of hydrogen is introduced into the working gas, correlated with the lowest resistivity achieved.

The surface morphology of ITO thin films was observed by SEM. Almost all the ITO films reveal a compact dense and granular structure regardless of process conditions, excluding the ITO films produced at an argon working pressure of 4.35 mTorr (ITORTp4.35) and 4.85 mTorr (ITORTp4.85). The latter ITO films reveal a smoother surface, with no clear evidence of well-defined small grains. This information is in good correlation with the XRD diffraction pattern and the results of the grain size using the Debye-Scherrer equation presented in Table 3, where it can be seen that higher Ar working pressures lead to an amorphous structure. The grain size slightly increases for ITO films produced at low Ar working pressures, but some voids are present. This can be explained by the higher energy of the sputtered species arriving at the substrate due to reduced number of collisions. However, increasing the substrate temperature to 250 °C or adding plasma irradiation with power up to 40 W or adding a partial pressure of hydrogen to the working gas, the surface morphology looks more texturized with a uniform distribution of grains, without voids. The composition of the ITO films has been measured by EDS and the average composition for all the samples were 7.89 at. % for In, 1.74 at. % for Sn and 31.65 at. % for O. The white particles on the surface of the films, identified with dashed red curves, were identified as pieces of carbon (as shown in the table presented in Figure 2), after the coating of the ITO films with a conductive material, in this case carbon, to increase the conductivity of the sample surface.

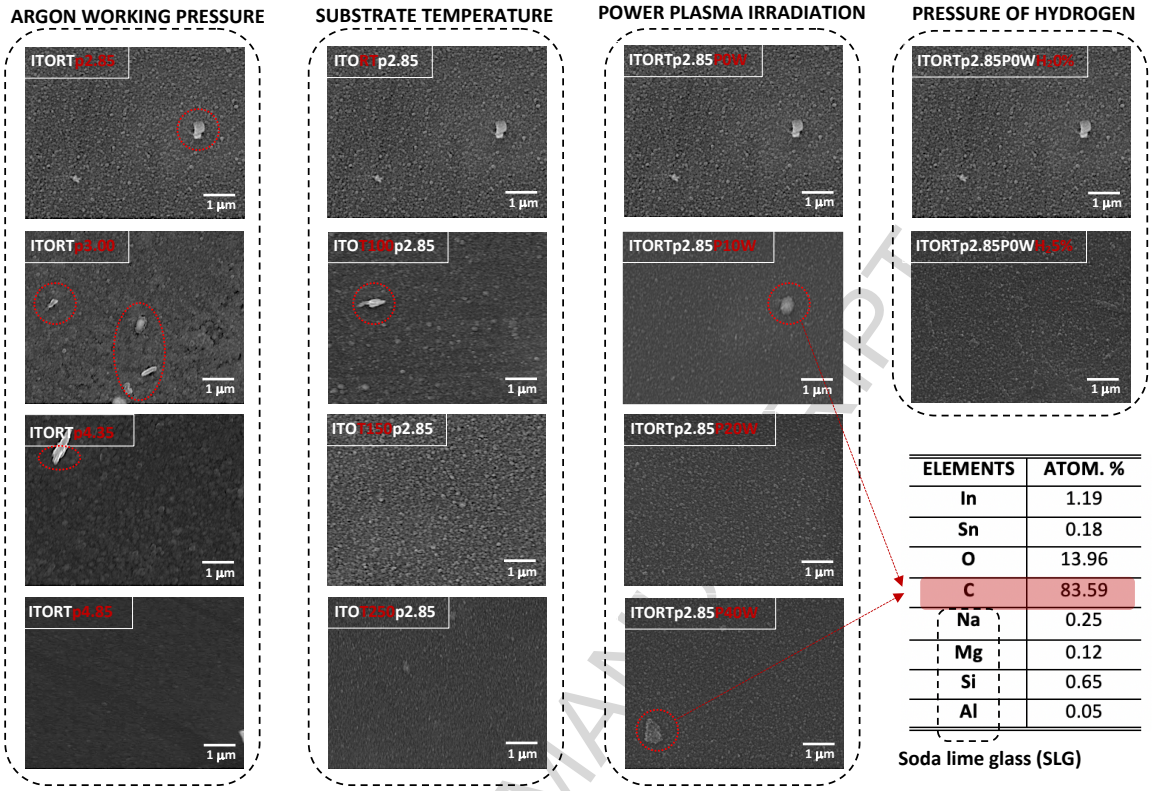

Figure 2: SEM micrographs of the top surface of the ITO films deposited under different a) Argon working pressures; (b) Substrate temperatures; (c) Plasma irradiation power and, (d) partial pressure of hydrogen to the working gas.

3.2. Electrical properties of ITO thin films

Figure 3 shows the eletrical properties of the ITO films. These results show that the resistivity gradually increased with increasing argon working pressure below 4.35 mTorr and then it increased abruptly. This is consistent with the observed decrease in the carrier concentration accompained by a decrease in the mobility. When the substrate temperature was increased the resistivity decreased for temperatures above 100 °C due to an increase in the hall mobility and carrier concentration. The decrease of resistivity with substrate temperature is correlated with the increase in the crystallinity of the films (as shown on figure 1 b)). As mentioned before, the high conductivity of the films results mainly from stoichiometric deviation and the conduction electrons in these films are supplied from donor sites associated with oxygen vacancies or excess metal ions [23, 33, 34, 35]. Mobility is said to increase due to enhanced crystallinity of the films deposited at higher substrate temperatures. Surprisingly as the substrate temperature was increased from RT to 100 °C the resistivity peaked due to an abrupt decrease in the charge carrier concentration. The results also show that a decrease in the deposition rate occurs as the substrate temperature is increased probably due the lowering of the sticking coefficient.

Regarding the plasma irradiation during growth, the results suggest that for power 10 W, the resistivity decreases dominated by the increase in carrier concentration. Above that power it decreases again due to the decrease in carrier concentration and mobility. Regarding the partial pressure of hydrogen, the results show that the resistivity decreases with the addition of a hydrogen partial pressure (5% H_2) dominated by the increase in carrier concentration and despite a slight decrease in hall mobility. The observed low mobility of ITO and its dependence on carrier concentration has been explained in terms of scattering mechanisms due

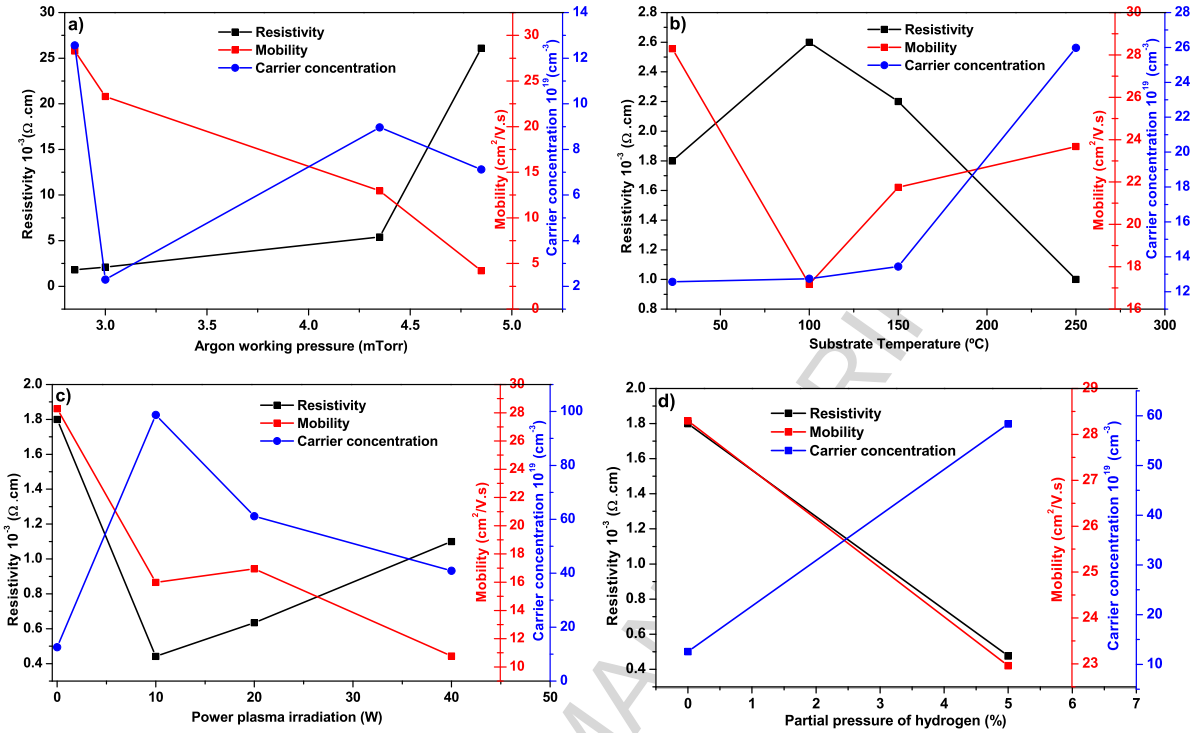

Figure 3: Electrical properties as a function of a) Argon working pressure; b) Substrate temperature; c) Power plasma irradiation and, d) Partial pressure of hydrogen.

to ionized impurities and grain boundaries [33, 34, 35]. The increase in carrier concentration with addition of hydrogen to the working gas can be explained by the ability of H_2 to remove oxygen from the films and because its interstitial incorporation is known to lead to additional donor states. As discussed for the case of increasing substrate temperature also for the cases of increasing plasma irradiation power and adding H_2 to the working gas led to the reduction of deposition rate as shown in the film thickness column of Table 3.

3.3. Optical properties of ITO thin films

The optical properties of a transparent conducting film depend strongly on the growth technique, deposition parameters, microstructure and level of impurities. Being transparent in the visible and consequent near-infrared region and reflecting to the infrared radiation, they act as selective transmiting layer [36]. Optical measurements were performed, from which the band gap energies were estimated (Figure 4). The absorption edge analysis of the ITO films shows that increasing the working pressure leads to a decrease in the band gap and the increase in the substrate temperature or addition of 5% of hydrogen to the working gas leads to an increase in the band gap. Increasing the plasma irradiation power of the growing films the values obtained for the band gap do not change substantially. All the values obtained are in the range of [3.5; 4.0] eV.

The transmittance spectral dependencies are given by the insets in Figure 4 and shows that with increasing the substrate temperature to 250 °C, decreasing the plasma irradiation power from 40 W to 10 W and adding hydrogen to the working gas, the transmittance at wavelengths above 1000 nm decreases. This is because of the free carrier absorption which increases as the carrier concentration increases.

In addition, the results above were compiled and joined together, resulting in the Table 3. The ITO samples with the low resistivity has been attributed to higher number of free electron [2] and for the

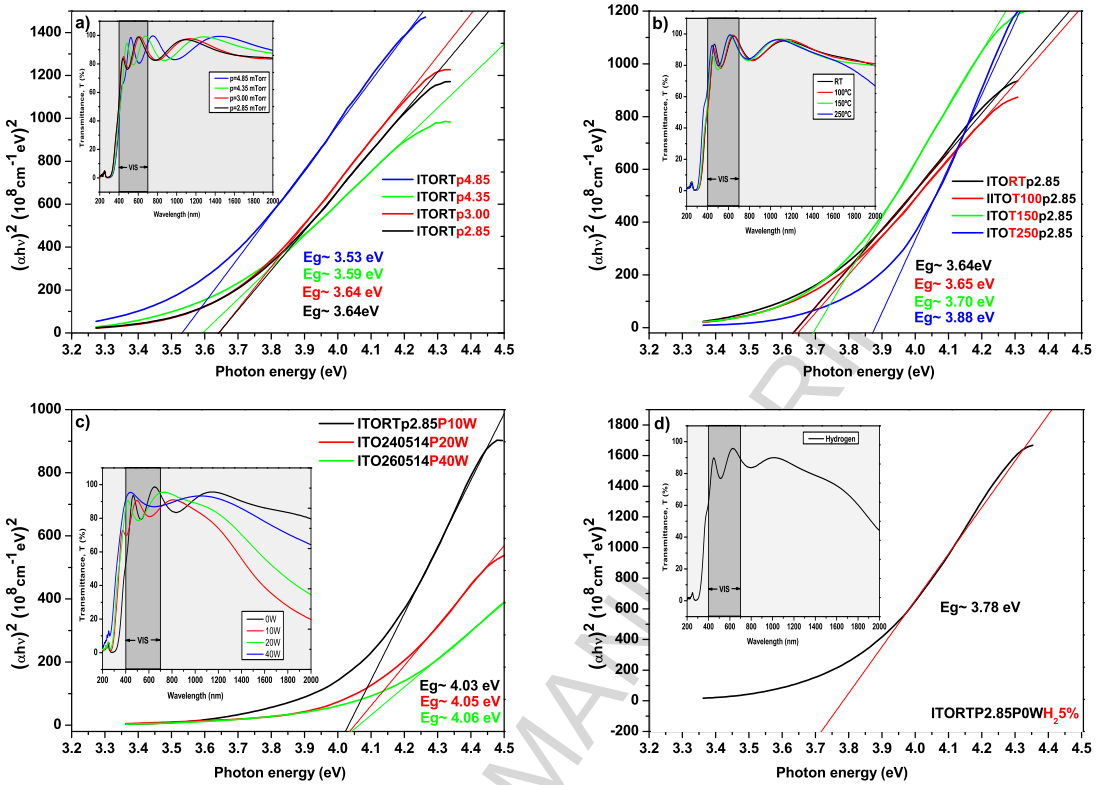

Figure 4: Optical properties as a function of a) Argon working pressure; b) Substrate temperature; c) Plasma irradiation power and, d) Partial pressure of hydrogen. In figures c) and d) for better accomodation of the results, the reference sample ITORTp2.85P0W or ITORTp2.85P0W$H_2$0% is not represented. Nevertheless, it is presented in figures a) and b) (ITORTp2.85).

equal sample for the four set of samples (ITORTp2.85) the value is $\sim$ 1.79x10^{20} cm^{-3}. Higher values are obtained, increasing the substrate temperature to 250 °C or applying a low plasma irradiation power or adding hydrogen to the working gas. All the values obtained for the band gap are in according to the values reported in literature [2, 4]. The correlation between the carrier concentration and apparent band gap values shows that the latter tends to increase with the former which is the result of the Moss-Burstein effect.

4. Conclusion

In this work we have explored how the properties of RF magentron sputtered ITO films were influenced by the set of deposition conditions. The main aim was establishing a practical route to obtain low resistivity and high transmittance films at low substrate temperature to avoid damaging temperature-sensitive substrates, such as, the heterointerface of thin film solar cells or polymeric ones. We studied the effect of the working pressure, the substrate temperature, the irradiation with a low power plasma during growth and the addition of a partial pressure of hydrogen to the working gas.

It was found that even though by reducing the working pressure it was possible to achieve low resistivity films by simultaneously increasing the carrier mobility and concentration, the most favorable route was found to be the addition of a partial pressure of hydrogen. The latter not only allowed us to achieve the second lowest resistivity of the ITO films obtained in this work, but it also reduced significantly the dependency of the films' properties on the target surface conditions. This latter aspect turned out to be very important in terms of the reduction of the target surface conditioning work required whenever the chamber was open for

Table 3: Main results for all the studied samples.

Samples	Thickness t (nm)	Grain size D (nm)	Sheet resistance $R_{\square}$ (Ω/sq)	Resistivity ρ (x10^{-4}) (Ω.cm)	Hall mobility μ_{Hall} ($cm^2/V.s$)	Carrier concentration n (x10^{20}) (cm^{-3})	Band gap E_{gap} (eV)
ITORTp2.85	349	25.3	35	12.0	26.9	1.79	3.64
ITORTp3.00	290	26.3	68	21.0	23.3	0.23	3.64
ITORTp4.35	348	Amorphous	190	54.0	12.9	0.89	3.59
ITORTp4.85	303	Amorphous	830	261	4.21	0.71	3.53
ITORTp2.85	349	25.3	35	12.0	26.9	1.79	3.64
ITOT100p2.85	362	24.4	74	26.0	17.2	1.27	3.65
ITOT150p2.85	298	23.3	71	22.0	21.7	1.34	3.70
ITOT250p2.85	285	24.2	34	10.0	23.7	2.59	3.88
ITORTp2.85P0W	349	25.3	35	12.0	26.9	1.79	3.64
ITORTp2.85P10W	274	13.3	31	6.34	16.9	6.11	4.03
ITORTp2.85P20W	248	11.5	23	4.41	15.9	9.87	4.06
ITORTp2.85P40W	192	0.62	59	11.0	10.8	4.09	4.05
ITORTp2.85P0W$H_2$0%	349	25.3	35	12.0	26.9	1.79	3.64
ITORTp2.85P0W$H_2$5%	248	26.3	23	4.76	22.9	5.83	3.78

target replacement or maintenance which means a substantially higher target material utilization percentage in actual devices.

The lowest resistivity was achieved by irradiating the growing ITO films with an Ar plasma at 20 W. This led to films in which the preferential orientation shifted from (222) to (400) and small crystallite size. The irradiation led to a pronounced increase in carrier concentration accompained by a decrease in mobility but still an overall reduction in resistivity. A drawback of this approach is that we do not control the real substrate temperature. Growth techniques and the sputtering environment play an important role in governing the properties of ITO thin films. This is because of the fact that the optical and electrical properties of the films strongly depend on the structure, morphology and nature of the impurities present, which depend on the method of preparation. The oxidation state and the impurity content affect the properties of ITO, since the oxidising or reducing conditions during deposition modify the oxygen vacancy content, thus modifying the carrier density.

The n-type conductivity of the ITO films has been attributed to both substitutional tin and oxygen vacancies, created during film growth resulting in a material represented as $In_{2-x}Sn_xO_{3-2x}$. The presence of hydrogen in the working gas is expected to remove oxygen from the ITO films promoting the formation of oxygen vacancies [37, 38]. It is also known that some intersticial incorporation of hydrogen into the ITO films leads to the formation of additional donor state. Indeed, our results show an increase in the carrier concentration by a factor of 3 with just a minor reduction in the mobility thus leading to an overall reduction in the resistivity without degrading substantially the transmittance. ITO films were produced very reproducibly with a thickness of 248 nm, displaying a sheet resistance of 23 Ω/sq and an average transmittance, in the visible range, of 90 %.

5. Acknowledgments

The authors acknowledge the financial support from the Portuguese Science and Technology Foundation (FCT), through the grant SFRH/BD/102807/2014. This work is also funded by FEDER funds through the COMPETE 2020 Programme and National funds through FCT under the project UID/CTM/50025/2013.

References

[1] T. O. M. T.J. Coutts, J.D. Perkins, and D.S. GinleyMason, Transparent Conducting Oxides : Status and Opportunities in Basic, Tech. Rep. August (1999).

[2] S. A. Knickerbocker, A. K. Kulkarni, Calculation of the figure of merit for indium tin oxide films based on basic theory, Journal of Vacuum Science & Technology A: Vacuum, Surfaces, and Films 13 (3) (1995) 1048–1052. doi:10.1116/1.579583.

[3] P. P. Edwards, A. Porch, M. O. Jones, D. V. Morgan, R. M. Perks, Basic materials physics of transparent conducting oxides, Dalton Transactions (19) (2004) 2995. doi:10.1039/b408864f.

[4] K. L. Chopra, S. Major, D. K. Pandya, Transparent conductors-A status review, Thin Solid Films 102 (1) (1983) 1–46. doi:10.1016/0040-6090(83)90256-0.

[5] P. Nath, R. F. Bunshah, Preparation of In2O3 and tin-doped In2O3 films by a novel activated reactive evaporation technique, Thin Solid Films 69 (1) (1980) 63–68. doi:10.1016/0040-6090(80)90204-7.

[6] T. Minami, Present status of transparent conducting oxide thin-film development for Indium-Tin-Oxide (ITO) substitutes, Thin Solid Films 516 (17) (2008) 5822–5828. doi:10.1016/j.tsf.2007.10.063.

[7] Y. Zhang, K. Eder, M. He, F. Liu, C. Yan, J. Huang, L. Yang, J. M. Cairney, X. Hao, H. Sun, A. Pu, S. Johnston, J. A. Stride, M. A. Green, K. Sun, S. Chen, N. J. Ekins-Daukes, Z. Hameiri, Cu2ZnSnS4 solar cells with over 10% power conversion efficiency enabled by heterojunction heat treatment, Nature Energy 3 (9) (2018) 764–772. doi:10.1038/s41560-018-0206-0.
URL http://dx.doi.org/10.1038/s41560-018-0206-0

[8] T. Kato, H. Hiroi, N. Sakai, S. Muraoka, H. Sugimoto, Characterization of front and back interfaces on Cu2ZnSnS4 thin-film solar cells 18 (201203046) (2012) 46–49. doi:10.3969/j.issn.1672-7193.2016.01.031.

[9] C. Zhang, J. Tao, J. Chu, An 8.7% efficiency co-electrodeposited Cu2 ZnSnS4 photovoltaic device fabricated via a pressurized post-sulfurization process, Journal of Materials Chemistry C (November). doi:10.1039/C8TC05058A.
URL http://xlink.rsc.org/?DOI=C8TC05058A

[10] B. Shin, O. Gunawan, Y. Zhu, N. A. Bojarczuk, S. J. Chey, S. Guha, Thin film solar cell with 8.4% power conversion efficiency using an earth-abundant Cu2ZnSnS4 absorber, Progress in Photovoltaics: Research and Applications 21 (2013) 72–76. doi:10.1002/pip.1174.

[11] F. Jiang, S. Ikeda, T. Harada, M. Matsumura, Pure Sulfide Cu2ZnSnS4thin film solar cells fabricated by preheating an electrodeposited metallic stack, Advanced Energy Materials 4 (7) (2014) 2–5. doi:10.1002/aenm.201301381.

[12] V. Tunuguntla, W.-C. Chen, P.-H. Shih, I. Shown, Y.-R. Lin, J.-S. Hwang, C.-H. Lee, L.-C. Chen, K.-H. Chen, A nontoxic solvent based solgel Cu 2 ZnSnS 4 thin film for high efficiency and scalable low-cost photovoltaic cells, Journal of Materials Chemistry A 3 (29) (2015) 15324–15330. doi:10.1039/C5TA02833G.
URL http://xlink.rsc.org/?DOI=C5TA02833G

[13] Y. S. Lee, T. Gershon, O. Gunawan, T. K. Todorov, T. Gokmen, Y. Virgus, S. Guha, Cu2ZnSnSe4 thin-film solar cells by thermal co-evaporation with 11.6% efficiency and improved minority carrier diffusion length, Advanced Energy Materials 5 (7) (2015) 2–5. doi:10.1002/aenm.201401372.

[14] G. Brammertz, M. Buffière, S. Oueslati, H. Elanzeery, K. Ben Messaoud, S. Sahayaraj, C. Köble, M. Meuris, J. Poortmans, Characterization of defects in 9.7% efficient Cu2ZnSnSe4-CdS-ZnO solar cells, Applied Physics Letters 103 (16). doi:10.1063/1.4826448.

[15] C. J. Hages, N. J. Carter, R. Agrawal, Generalized quantum efficiency analysis for non-ideal solar cells: Case of Cu2ZnSnSe4, Journal of Applied Physics 119 (1). doi:10.1063/1.4939487.
URL http://dx.doi.org/10.1063/1.4939487

[16] W. Wang, M. T. Winkler, O. Gunawan, T. Gokmen, T. K. Todorov, Y. Zhu, D. B. Mitzi, Device characteristics of CZTSSe thin-film solar cells with 12.6% efficiency, Advanced Energy Materials 4 (7) (2014) 1301465. doi:10.1002/aenm.201301465.
URL http://onlinelibrary.wiley.com/doi/10.1002/aenm.201301465/fullhttp://doi.wiley.com/10.1002/aenm.201301465

[17] W. Wu, N. G. Tassi, Y. Cao, J. V. Caspar, K. Roy-Choudhury, L. Zhang, Optoelectronic characteristics of >9% efficient bilayered CuZnSn(S,Se)<inf>4</inf> photovoltaic device, Physica Status Solidi - Rapid Research Letters 9 (4) (2015) 236–240. doi:10.1002/pssr.201510048.

[18] F. Liu, F. Zeng, N. Song, L. Jiang, Z. Han, Z. Su, C. Yan, X. Wen, X. Hao, Y. Liu, Kesterite Cu<inf>2</inf>ZnSn(S,Se)<inf>4</inf> Solar Cells with beyond 8% Efficiency by a Sol-Gel and Selenization Process, ACS Applied Materials and Interfaces 7 (26) (2015) 14376–14383. doi:10.1021/acsami.5b01151.

[19] G. Altamura, M. Wang, K. L. Choy, Influence of alkali metals (Na, Li, Rb) on the performance of electrostatic spray-assisted vapor deposited Cu2 ZnSn(S,Se)4 solar cells, Scientific Reports 6 (February) (2016) 1–9. doi:10.1038/srep22109.
URL http://dx.doi.org/10.1038/srep22109

[20] J. Kim, H. Hiroi, T. K. Todorov, O. Gunawan, M. Kuwahara, T. Gokmen, D. Nair, M. Hopstaken, B. Shin, Y. S. Lee, W. Wang, H. Sugimoto, D. B. Mitzi, High efficiency Cu2ZnSn(S,Se)4 solar cells by applying a double in 2S3/CdS Emitter, Advanced Materials 26 (44) (2014) 7427–7431. doi:10.1002/adma.201402373.

[21] N. Manavizadeh, F. A. Boroumand, E. Asl-Soleimani, F. Raissi, S. Bagherzadeh, A. Khodayari, M. A. Rasouli, Influence of substrates on the structural and morphological properties of RF sputtered ITO thin films for photovoltaic application, Thin Solid Films 517 (7) (2009) 2324–2327. doi:10.1016/j.tsf.2008.11.027.

[22] M. Yamaguchi, A. Ide-Ektessabi, H. Nomura, N. Yasui, Characteristics of indium tin oxide thin films prepared using electron beam evaporation, Thin Solid Films 447-448 (2004) 115–118. doi:10.1016/j.tsf.2003.09.033.

[23] K. Sreenivas, S. Rao, A. Mansingh, Preparation and characterization of rf sputtered indium tin oxide films, Journal of Physics 15 (2) (1985) 384–392.

[24] J. Manifacier, L. Szepessy, J. F. Bresse, M. Perotin, In203 : (Sn) and SnO2: (F) F ilms - Application to soalr energy conversion part II- Electrical and Optical Properties 14 (c) (1979) 163–175. doi:https://doi.org/10.1016/0025-5408(79)90115-6.

[25] B. Mayer, Highly conductive and transparent films of tin and fluorine doped indium oxide produced by APCVD, Thin Solid Films 221 (1-2) (1992) 166–182. doi:10.1016/0040-6090(92)90811-0.

[26] S. A. Agnihotry, K. K. Saini, T. K. Saxena, K. C. Nagpal, S. Chandra, Studies on e-beam deposited transparent conductive

films of In 2 O 3 :Sn at moderate substrate temperatures, Journal of Physics D: Applied Physics 18 (10) (1985) 2087–2096. doi:10.1088/0022-3727/18/10/019.

[27] S. Ishibashi, Y. Higuchi, Y. Ota, K. Nakamura, Low resistivity indiumtin oxide transparent conductive films. II. Effect of sputtering voltage on electrical property of films, Journal of Vacuum Science & Technology A: Vacuum, Surfaces, and Films 8 (3) (1990) 1403–1406. doi:10.1116/1.576890.

[28] F. Kurdesau, G. Khripunov, A. F. da Cunha, M. Kaelin, A. N. Tiwari, Comparative study of ITO layers deposited by DC and RF magnetron sputtering at room temperature, Journal of Non-Crystalline Solids 352 (9-20 SPEC. ISS.) (2006) 1466–1470. doi:10.1016/j.jnoncrysol.2005.11.088.

[29] M. Clement, J. Santamaria, E. Iborra, G. González-Diaz, Effects of residual gases and rf power on ITO rf sputtered thin films, Vacuum 37 (5-6) (1987) 447–449. doi:10.1016/0042-207X(87)90333-2.

[30] H. Kim, J. Horwitz, A. Piqué, C. Gilmore, D. Chrisey, Electrical and optical properties of indium tin oxide thin films grown by pulsed laser deposition, Applied Physics A: Materials Science & Processing 69 (7) (1999) S447–S450. doi:10.1007/s003390051435.

[31] C. V. Vasant Kumar, A. Mansingh, Effect of target-substrate distance on the growth and properties of rf-sputtered indium tin oxide films, Journal of Applied Physics 65 (3) (1989) 1270–1280. doi:10.1063/1.343022.

[32] V. Mote, Y. Purushotham, B. Dole, Williamson-Hall analysis in estimation of lattice strain in nanometer-sized ZnO particles, Journal of Theoretical and Applied Physics 6 (1) (2012) 2–9. doi:10.1186/2251-7235-6-6.

[33] J. Bardeen, W. Shockley, Deformation potentials and mobilities in non-polar crystals, Physical Review 80 (1) (1950) 72–80. doi:10.1103/PhysRev.80.72.

[34] A. R. Hutson, Piezoelectric scattering and phonon drag in ZnO and CdS, Journal of Applied Physics 32 (10) (1961) 2287–2292. doi:10.1063/1.1777061.

[35] H. Ehrenreich, Band structure and transport properties of some 3-5 compounds, Journal of Applied Physics 32 (10) (1961) 2155–2166. doi:10.1063/1.1777035.

[36] N. M., Growth and Characterisation of Radio Frequency Magnetron Sputtered Indium Tin Oxide Thin Films, Ph.D. thesis (2006).

[37] Y.-L. Lee, K.-M. Lee, Effect of Ambient Gases on the Characteristics of ITO Thin Films for OLEDs, Transactions on Electrical and Electronic Materials 10 (6) (2009) 203–207. doi:10.4313/TEEM.2009.10.6.203.

[38] S. Luo, S. Kohiki, K. Okada, F. Shoji, T. Shishido, Hydrogen effects on crystallinity, photoluminescence, and magnetization of indium tin oxide thin films sputter-deposited on glass substrate without heat treatment, Physica Status Solidi (A) Applications and Materials Science 207 (2) (2010) 386–390. doi:10.1002/pssa.200925375.

Graphical abstract

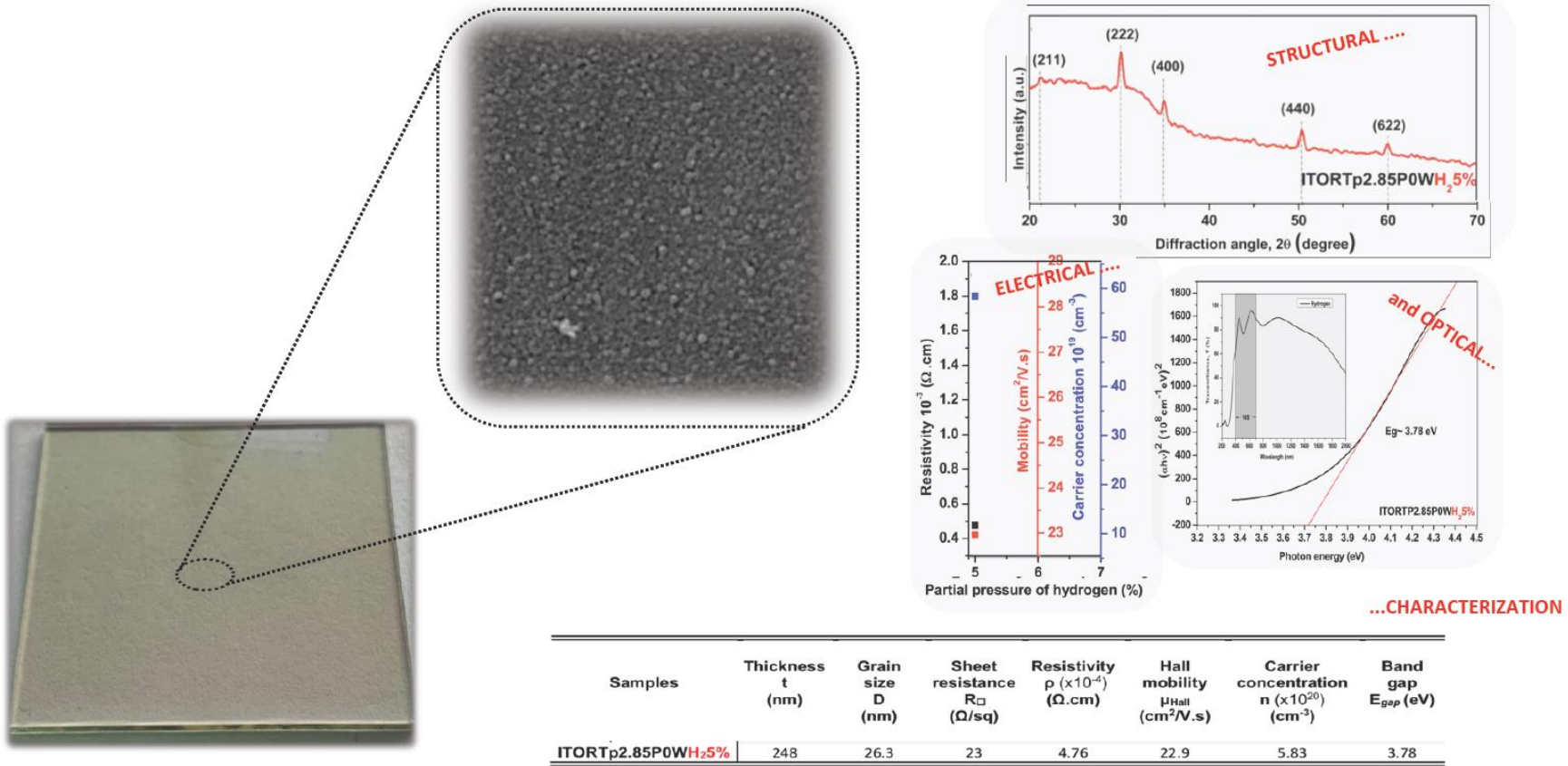

Samples	Thickness t (nm)	Grain size D (nm)	Sheet resistance $R_{\square}$ (Ω/sq)	Resistivity ρ (x10^{-4}) (Ω.cm)	Hall mobility μ_{Hall} (cm^2/V.s)	Carrier concentration n (x10^{20}) (cm^{-3})	Band gap E_{gap} (eV)
ITORTp2.85P0W$H_2$5%	248	26.3	23	4.76	22.9	5.83	3.78

Highlights

- Optimization of low temperature RF-magnetron sputtering of Indium Tin Oxide Films.
- We studied the effect of working pressure, temperature, plasma irradiation and H_2.
- The favorable route was found to be the addition of a partial pressure of H_2.
- ITO film with 248nm, 23Ω and a transmittance of 90%, in visible range was produced.

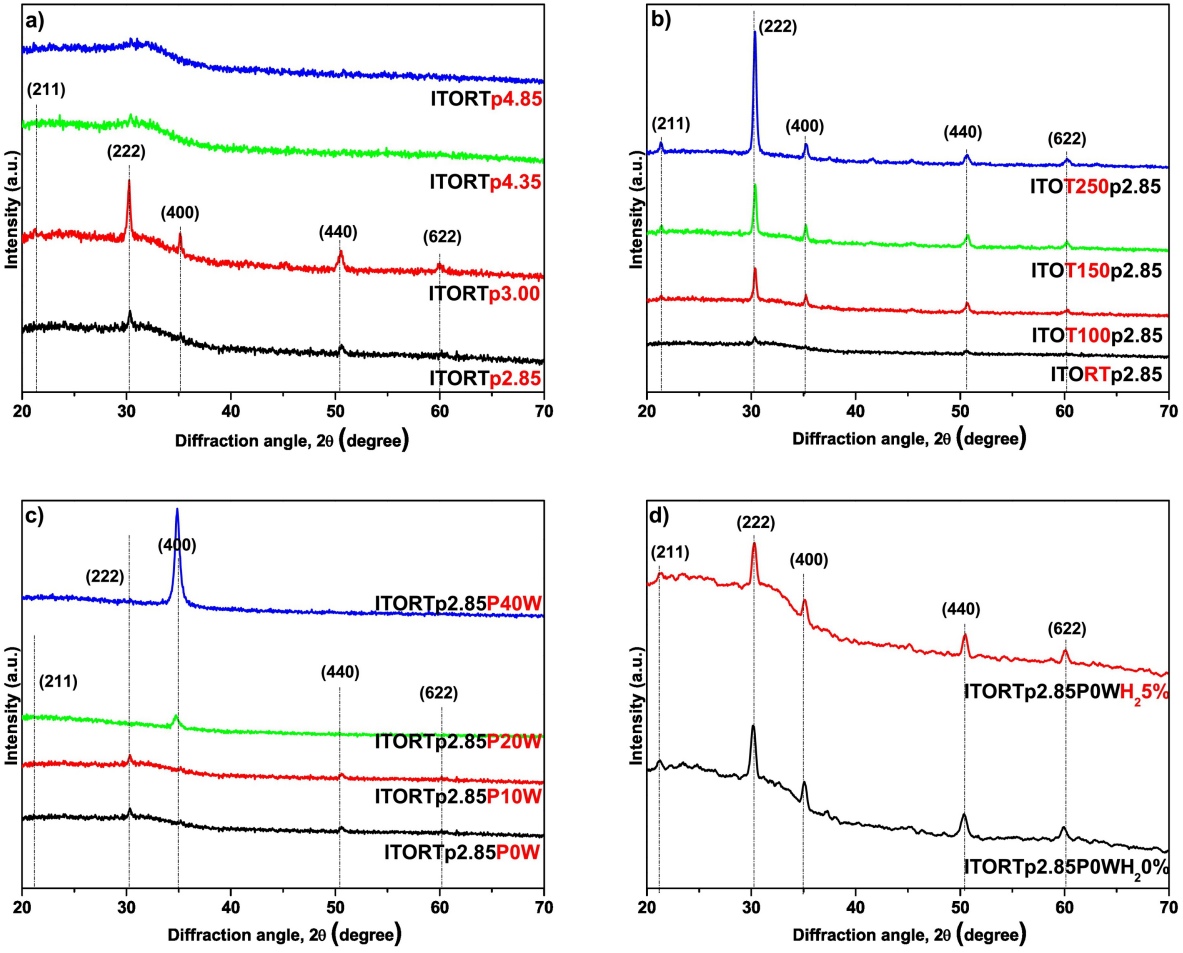
a)
(211)
(222)
(400)
(440)
(622)
ITORTp4.85
ITORTp4.35
ITORTp3.00
ITORTp2.85
Intensity (a.u.)
Diffraction angle, 2θ (degree)
b)
(222)
(211)
(400)
(440)
(622)
ITOT250p2.85
ITOT150p2.85
ITOT100p2.85
ITORTp2.85
Intensity (a.u.)
Diffraction angle, 2θ (degree)
c)
(400)
(222)
(211)
(440)
(622)
ITORTp2.85P40W
ITORTp2.85P20W
ITORTp2.85P10W
ITORTp2.85P0W
Intensity (a.u.)
Diffraction angle, 2θ (degree)
d)
(222)
(211)
(400)
(440)
(622)
ITORTp2.85P0WH2 5%
ITORTp2.85P0WH2 0%
Intensity (a.u.)
Diffraction angle, 2θ (degree)

Figure 1

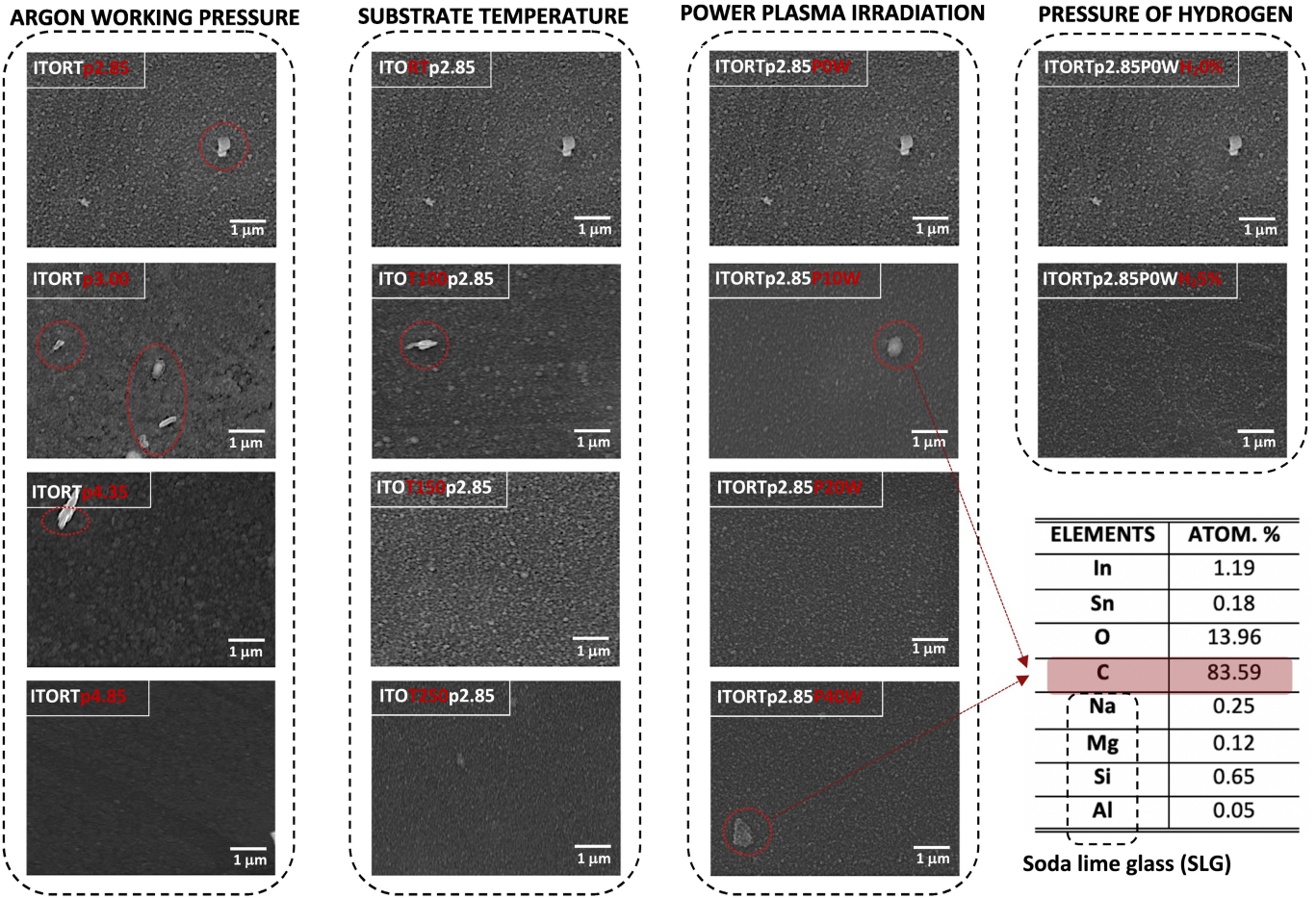

ELEMENTS	ATOM. %
In	1.19
Sn	0.18
O	13.96
C	83.59
Na	0.25
Mg	0.12
Si	0.65
Al	0.05

Soda lime glass (SLG)

Figure 2

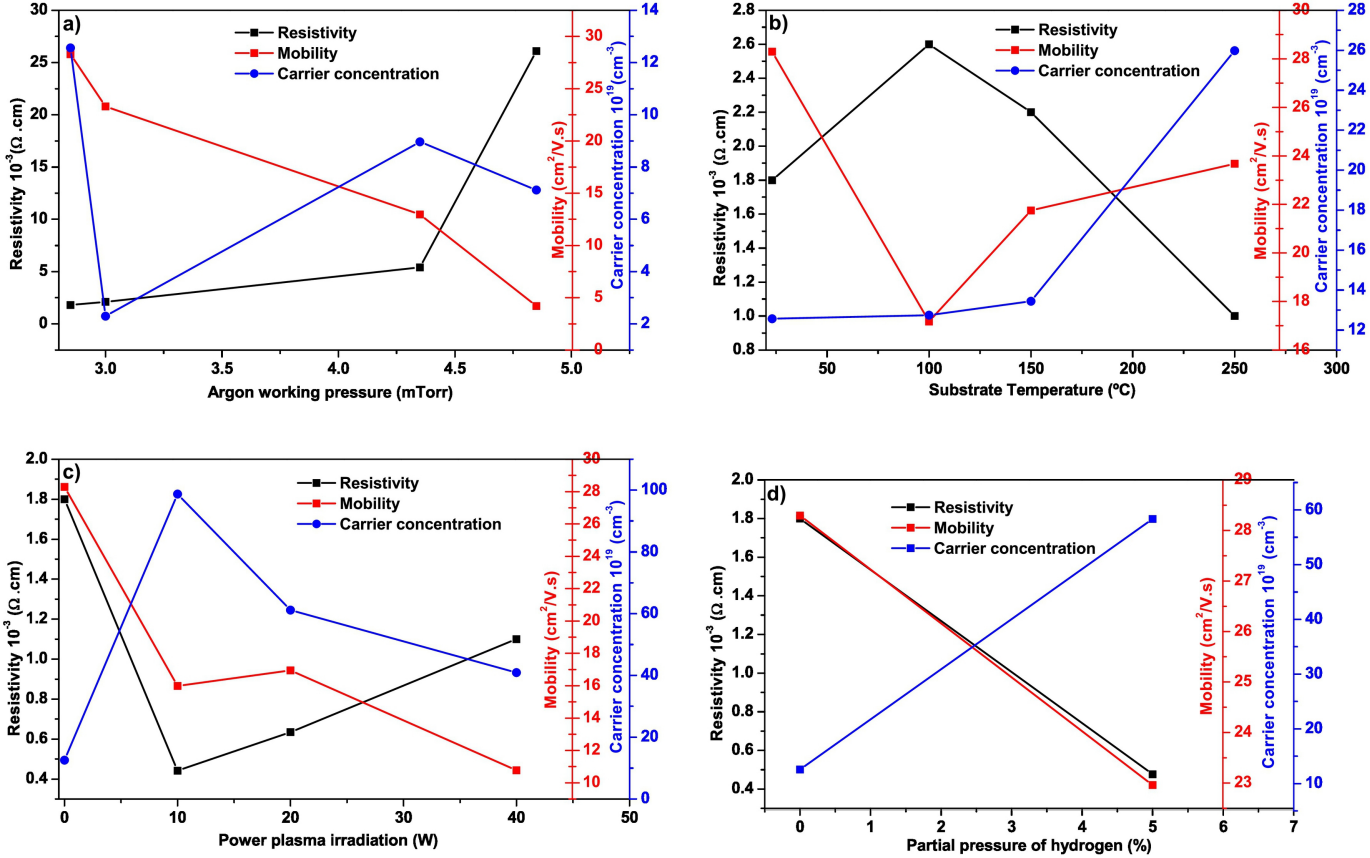
a)
Resistivity
Mobility
Carrier concentration
Resistivity 10^-3 (Ω.cm)
Mobility (cm^2/V.s)
Carrier concentration 10^19 (cm^-3)
Argon working pressure (mTorr)
b)
Resistivity
Mobility
Carrier concentration
Resistivity 10^-3 (Ω.cm)
Mobility (cm^2/V.s)
Carrier concentration 10^19 (cm^-3)
Substrate Temperature (°C)
c)
Resistivity
Mobility
Carrier concentration
Resistivity 10^-3 (Ω.cm)
Mobility (cm^2/V.s)
Carrier concentration 10^19 (cm^-3)
Power plasma irradiation (W)
d)
Resistivity
Mobility
Carrier concentration
Resistivity 10^-3 (Ω.cm)
Mobility (cm^2/V.s)
Carrier concentration 10^19 (cm^-3)
Partial pressure of hydrogen (%)

Figure 3

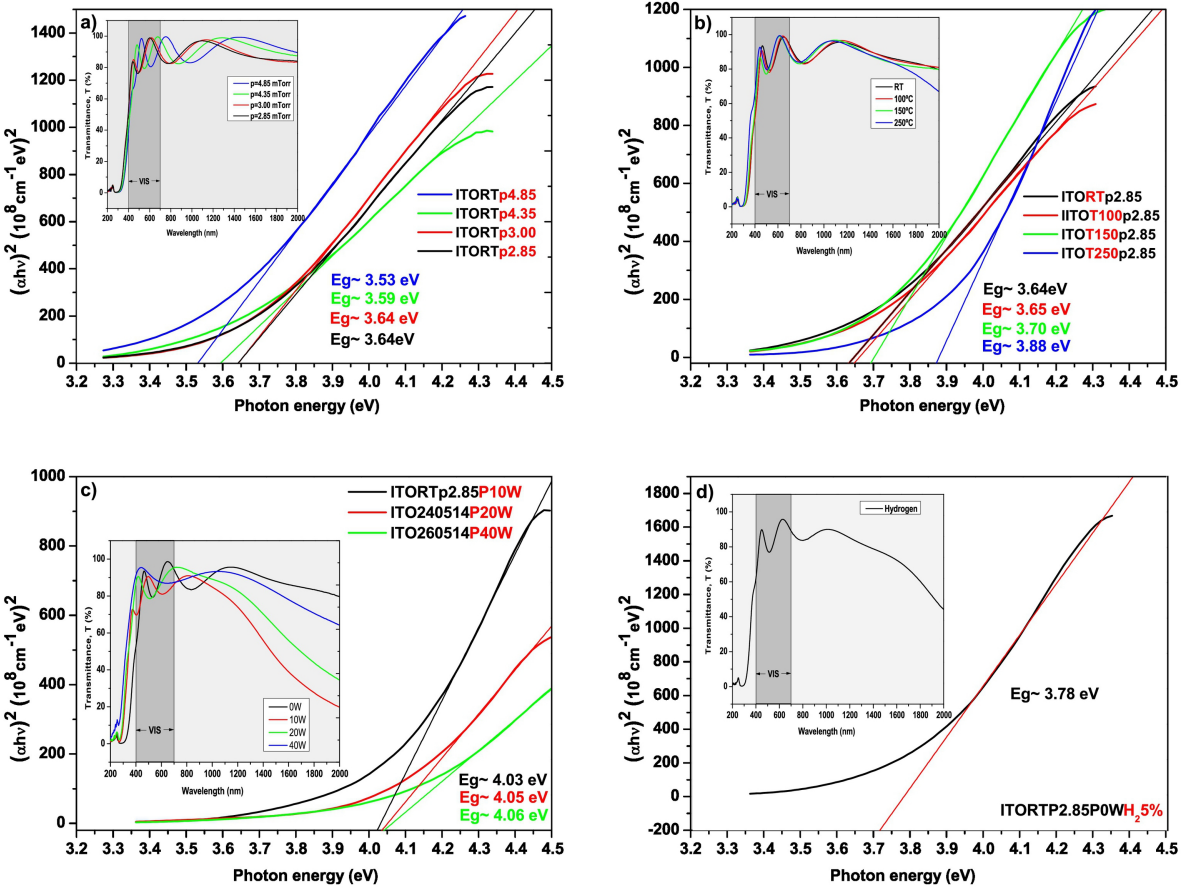
a)
p=4.85 mTorr
p=4.35 mTorr
p=3.00 mTorr
p=2.85 mTorr
Transmittance, T (%)
Wavelength (nm)
VIS
ITORTp4.85
ITORTp4.35
ITORTp3.00
ITORTp2.85
Eg~ 3.53 eV
Eg~ 3.59 eV
Eg~ 3.64 eV
Eg~ 3.64eV
(αhν)2 (10^8 cm^-1 eV)^2
Photon energy (eV)
b)
RT
100°C
150°C
250°C
ITORTp2.85
IITOT100p2.85
ITOT150p2.85
ITOT250p2.85
Eg~ 3.64eV
Eg~ 3.65 eV
Eg~ 3.70 eV
Eg~ 3.88 eV
c)
ITORTp2.85P10W
ITO240514P20W
ITO260514P40W
0W
10W
20W
40W
Eg~ 4.03 eV
Eg~ 4.05 eV
Eg~ 4.06 eV
d)
Hydrogen
Eg~ 3.78 eV
ITORTP2.85P0WH2 5%

Figure 4